PROTEIN DESIGN

Designed protein logic to target cells with precise combinations of surface antigens

Marc J. Lajoie[1,2]*†‡, Scott E. Boyken[1,2]*‡, Alexander I. Salter[3,4]*, Jilliane Bruffey[1,2,5], Anusha Rajan[3,4], Robert A. Langan[1,2]‡, Audrey Olshefsky[1,6], Vishaka Muhunthan[3,4], Matthew J. Bick[1,2]‡, Mesfin Gewe[4], Alfredo Quijano-Rubio[1,2,6], JayLee Johnson[1], Garreck Lenz[1], Alisha Nguyen[1], Suzie Pun[6,7], Colin E. Correnti[4], Stanley R. Riddell[3,4,8], David Baker[1,2,9]†

Precise cell targeting is challenging because most mammalian cell types lack a single surface marker that distinguishes them from other cells. A solution would be to target cells using specific combinations of proteins present on their surfaces. In this study, we design colocalization-dependent protein switches (Co-LOCKR) that perform AND, OR, and NOT Boolean logic operations. These switches activate through a conformational change only when all conditions are met, generating rapid, transcription-independent responses at single-cell resolution within complex cell populations. We implement AND gates to redirect T cell specificity against tumor cells expressing two surface antigens while avoiding off-target recognition of single-antigen cells, and three-input switches that add NOT or OR logic to avoid or include cells expressing a third antigen. Thus, de novo designed proteins can perform computations on the surface of cells, integrating multiple distinct binding interactions into a single output.

Biological systems are complex; therefore, interventions that perturb these systems must achieve specific targeting in mixed populations of closely related cells. Cells displaying a specific surface marker can be targeted with antibodies, but a single marker is rarely sufficient to identify specific cell types. Bispecific antibodies can achieve some selectivity by simultaneously engaging two targets (*1*, *2*), but this strategy requires delicate tuning of the individual binding affinities to reduce interactions with cells expressing just one of the targets. A generalized approach for distinguishing cells using combinations of surface markers is needed. Toward this end, we sought to develop a modular protein system capable of taking multiple binding events as input, computing combinations of Boolean logic operations (AND, OR, and NOT) without requiring cellular machinery for signal integration, and producing a single output (Fig. 1A).

How does one design a system that activates only on the surface of a cell and not in solution? Given that antigen binding at the cell surface increases the local concentration of the bound protein, such a system potentially could be constructed from an actuator that responds to proximity. To be generally useful, the actuation must be modular and independent of target antigen identity. We began from de novo designed protein switches that activate in solution: latching orthogonal cage–key protein (LOCKR) (*3*) switches consist of a structural "cage" protein that uses a "latch" domain to sequester a functional peptide in an inactive conformation until binding of a separate "key" protein induces a conformational change that enables binding to an effector protein. Cage, key, and effector bind in a three-way equilibrium, and the sensitivity of the switch can be tuned by adjusting the relative cage–latch and cage–key affinities. Previous LOCKR switches functioned in the yeast cytoplasm (*3*) but were aggregation-prone once purified, likely because of domain swapping of symmetric repeats inherited from the parental α-helical homotrimer (*4*). To alleviate aggregation, we used Rosetta (*5*) to design a new LOCKR switch with shorter helices, improved hydrophobic packing, and an additional hydrogen bond network to promote interaction specificity among the helices (fig. S1, see the computational protein design section of the supplementary materials). The new design was nearly 100% monomeric (fig. S2, top), and a 2.1-Å x-ray crystal structure [Protein Data Bank (PDB) ID 7JH5] closely matched the design model (Fig. 1B and table S1) with a root mean square deviation (RMSD) of 1.1 Å across all backbone atoms and an RMSD of 0.5 Å across all sidechain heavy atoms in the newly designed hydrogen bond network (Fig. 1B).

To install an output function into colocalization-dependent LOCKR (Co-LOCKR), we chose the Bim-Bcl2 pair as a model system (Bcl2, B cell lymphoma 2; Bim, Bcl2-interacting mediator of cell death) (*6*). Bim was encoded into the latch as a sequestered peptide, and Bcl2 was used as the effector. We added targeting domains that recruit the Co-LOCKR cage and key to cells expressing target antigens. While the targeting domains should bind to any cell expressing their target antigens, only cells with both antigens should colocalize cage and key (Fig. 1C). Because Co-LOCKR is thermodynamically controlled, complex formation occurs at much lower solution concentrations when the components are bound to and colocalized on a surface than when they are unbound (fig. S3, A and B); colocalization shifts the binding equilibrium in favor of complex formation (fig. S3C).

To evaluate the ability of Co-LOCKR to target cells coexpressing a precise combination of surface antigens, we developed a mixed-population flow cytometry assay by combining four K562 cell lines expressing Her2-eGFP, EGFR-iRFP, both, or neither (eGFP, enhanced green fluorescent protein; EGFR, epidermal growth factor receptor; iRFP, near-infrared fluorescent protein) (Fig. 1D). We used designed ankyrin repeat protein (DARPin) domains (*7*, *8*) to target the cage and key to Her2 and EGFR, respectively. If the system functions as designed, only cells coexpressing both Her2 and EGFR should activate Co-LOCKR and bind Bcl2 (Fig. 1E): The cage contains the sequestered Bim peptide, and the key is required for its exposure. We refer to this Co-LOCKR configuration as CL_C_HK_E; in this nomenclature, CL refers to Co-LOCKR, C_H indicates that the cage is targeted to Her2, and K_E indicates that the key is targeted to EGFR (table S2). When the mixed population of cells was coincubated with an equimolar dilution series of cage and key (3 μM to 1.4 nM) and washed before adding AlexaFluor594-labeled Bcl2 (Bcl2-AF594), the expected sigmoidal binding curve was observed for the Her2-EGFR cells but not for cells expressing either antigen alone (Fig. 1, F and G).

We next sought to tune the dynamic range of Co-LOCKR activation to increase colocalization-dependent activation sensitivity and responsiveness. The sensitivity of previous LOCKR switches was tuned by shortening the latch to produce a "toehold," which allows the key to outcompete the latch (*3*), but this also promoted aggregation (fig. S2, bottom). We therefore focused on designing mutations rather than toeholds to tune the relative interaction affinities of the Co-LOCKR system to be colocalization dependent (fig. S4). We mutated large, hydrophobic residues in the latch [Ile^{287}→Ala (I287A), I287S, I269S] or cage (L209A) to weaken cage–latch affinity (Fig. 2A). Biolayer

[1]Institute for Protein Design, University of Washington, Seattle, WA, USA. [2]Department of Biochemistry, University of Washington, Seattle, WA, USA. [3]Immunotherapy Integrated Research Center, Fred Hutchinson Cancer Research Center, Seattle, WA, USA. [4]Clinical Research Division, Fred Hutchinson Cancer Research Center, Seattle, WA, USA. [5]Graduate Program in Molecular and Cellular Biology, University of Washington, Seattle, WA, USA. [6]Department of Bioengineering, University of Washington, Seattle, WA, USA. [7]Molecular Engineering and Sciences Institute, University of Washington, Seattle, WA, USA. [8]Department of Medicine, University of Washington School of Medicine, Seattle, WA, USA. [9]Howard Hughes Medical Institute, University of Washington, Seattle, WA, USA.
*These authors contributed equally to this work.
†Corresponding author. Email: mlajoie@lyell.com (M.J.L.); dabaker@uw.edu (D.B.) ‡Present address: Lyell Immunopharma, Inc., Seattle, WA, USA.

interferometry indicated that increasingly disruptive mutations improved responsiveness (fig. S5, A and B), and flow cytometry showed that tuning the cage–latch interface enhanced colocalization-dependent signal without compromising specificity (Fig. 2B and fig. S5C). Colocalization-dependent activation occurred even at low nanomolar concentrations of CL_C_HK_E (fig. S5, D and E). Very little effector binding was observed for cells expressing Her2 or EGFR alone, confirming that Co-LOCKR has single-cell targeting resolution in a mixed population. Of the switches tested, I269S exhibited the greatest activation (fig. S6A), the parental Co-LOCKR design exhibited the lowest off-target activation (fig. S6B), and I287A exhibited the highest specificity (on-target signal divided by max off-target signal) (fig. S6C).

Colocalization-dependent activation was observed further at the subcellular level by

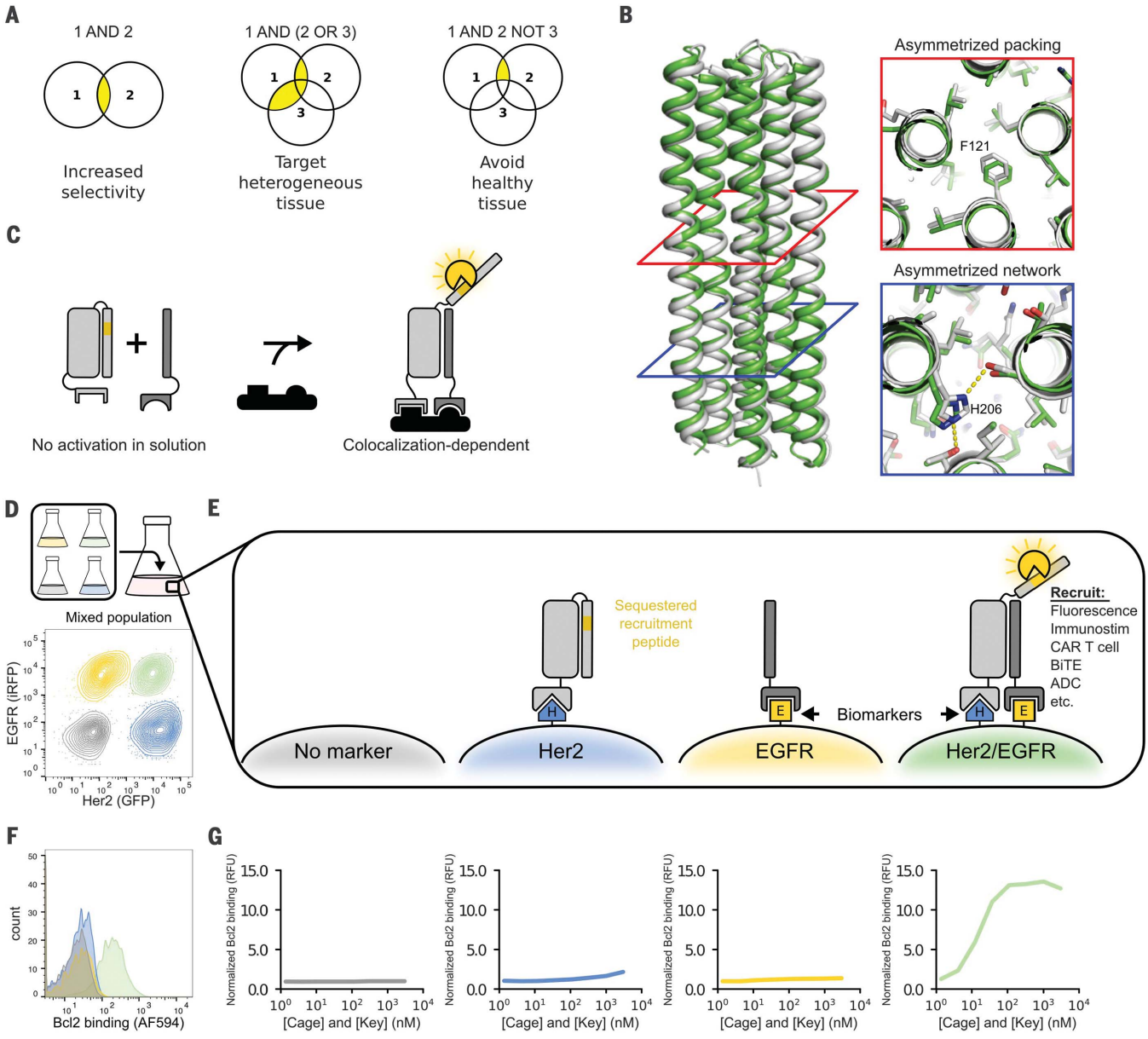

Fig. 1. A de novo designed protein switch performs AND logic on the cell surface. (**A**) The ability to compute logic operations on the surface of cells enables more precise targeting. (**B**) Structure of cage design used to create Co-LOCKR; the x-ray crystal structure (white, PDB ID 7JH5) matches the computational design model (green) with an RMSD of 1.1 Å across all backbone atoms. Cross sections illustrate asymmetric packing of hydrophobic residues (red square) and an asymmetric hydrogen bond network (blue square). F, Phe; H, His. (**C**) Colocalization-dependent protein switches are tuned so that cage and key do not interact in solution but strongly interact when colocalized on a surface by way of targeting domains. (**D**) Flow cytometry discriminates $Her2^+EGFR^+$ cells in a mixed population of K562 cells expressing Her2-eGFP (blue), EGFR-iRFP (yellow), both (green), or neither (gray). (**E**) An effector protein is recruited only when cage and key are colocalized on the surface of the same cell (AND logic). (**F**) The mixed population of cells from (D) was incubated with 111 nM Her2-targeted cage, 111 nM EGFR-targeted key, and 50 nM Bcl2-AF594. Bcl2 binding was only observed for the $Her2^+EGFR^+$ cells. (**G**) The mixed population of cells from (D) was incubated with a dilution series of Her2-targeted cage and EGFR-targeted key, washed, and then incubated with 50 nM Bcl2-AF594. Bcl2 binding is reported relative to K562 cells incubated with 3000 nM Her2-targeted cage, 3000 nM EGFR-targeted key, and 50 nM Bcl2-AF594. RFU, relative fluorescence units.

confocal microscopy. CL_C_HK_E recruited Bcl2-AF680 to the plasma membrane of Her2$^+$EGFR$^+$, but not Her2$^+$ or EGFR$^+$ human embryonic kidney 293T (HEK293T) cells (Fig. 2C). Co-LOCKR activation levels correlated with the extent of Her2-eGFP and EGFR-iRFP colocalization on the plasma membrane (Fig. 2D).

To assess the flexibility of Co-LOCKR, we attempted to specifically target alternative pairwise combinations of three cancer-associated antigens [Her2, EGFR, and EpCAM (epithelial cell adhesion molecule)]. Each of these antigens are expressed at differing levels by engineered K562 cell lines or human cancer cell lines (figs. S7A and S8A and table S3). Using the I269S variant to maximize detection of low levels of antigen, (i) Co-LOCKR distinguished the correct pair of antigens in every case, and (ii) the magnitude of Bcl2 binding corresponded with the expression level of the less-expressed of the two target antigens (Fig. 3A and fig. S8, B and C), consistent with a stoichiometric binding mechanism for colocalization-dependent activation. Together, these results demonstrate the modularity of Co-LOCKR to target several antigens expressed at differing levels. Although we

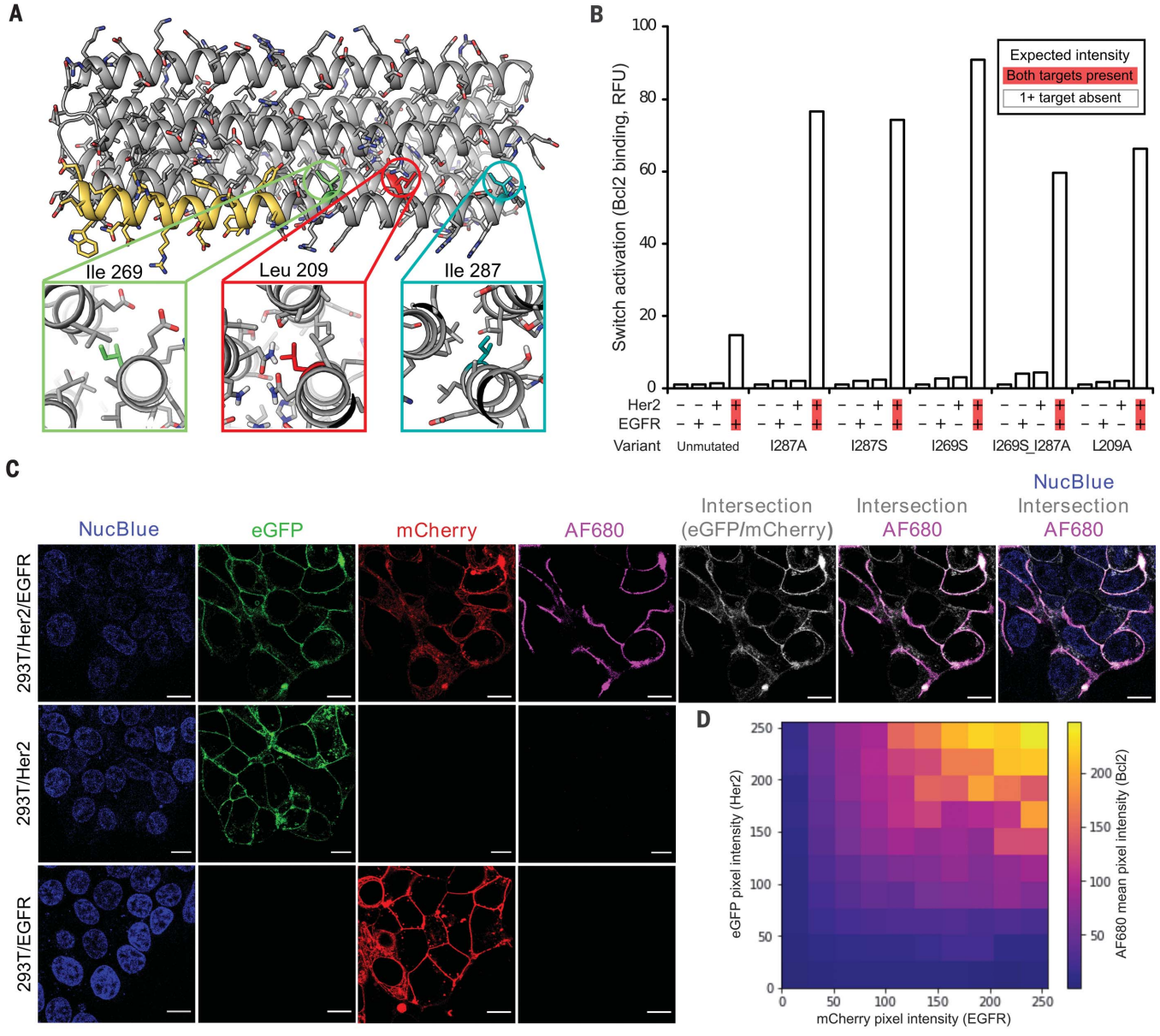

Fig. 2. Tuning Co-LOCKR sensitivity. (**A**) Design model of Co-LOCKR with the Bim functional peptide in yellow. Three buried hydrophobic amino acids were mutated to Ala or Ser to weaken the cage–latch affinity, thereby favoring cage–key binding. (**B**) Tuned Co-LOCKR variants exhibit greater colocalization-dependent activation than the unmutated parental variant. CL_C_HK_E variants recruiting Bcl2-AF594 were evaluated by flow cytometry using the mixed population of cells from Fig. 1D. The data shown represent 12.3 nM CL_C_HK_E (n = 1), and fig. S5C shows the complete dilution series for each variant. S, Ser; L, Leu. (**C**) Confocal microscopy of HEK293T cell lines shows that Co-LOCKR switches recruit Bcl2-AF680 effector proteins only where Her2 and EGFR are colocalized. Each cell line was incubated with CL_C_HK_E (I269S cage) and Bcl2-AF680 before imaging. NucBlue is a nuclear stain, eGFP indicates Her2 localization, mCherry indicates EGFR localization, AF680 indicates Bcl2 binding in response to Co-LOCKR activation, and white indicates the intersection of Her2-eGFP and EGFR-mCherry signal. Scale bars, 10 μm. See fig. S16, A to C, for uncropped versions of these images. (**D**) Heatmap showing the intensity of AF680 signal (Co-LOCKR activation) versus eGFP (Her2) and mCherry (EGFR) pixel intensity. Calculations were based on the uncropped 293T-Her2-EGFR image in fig. S16A.

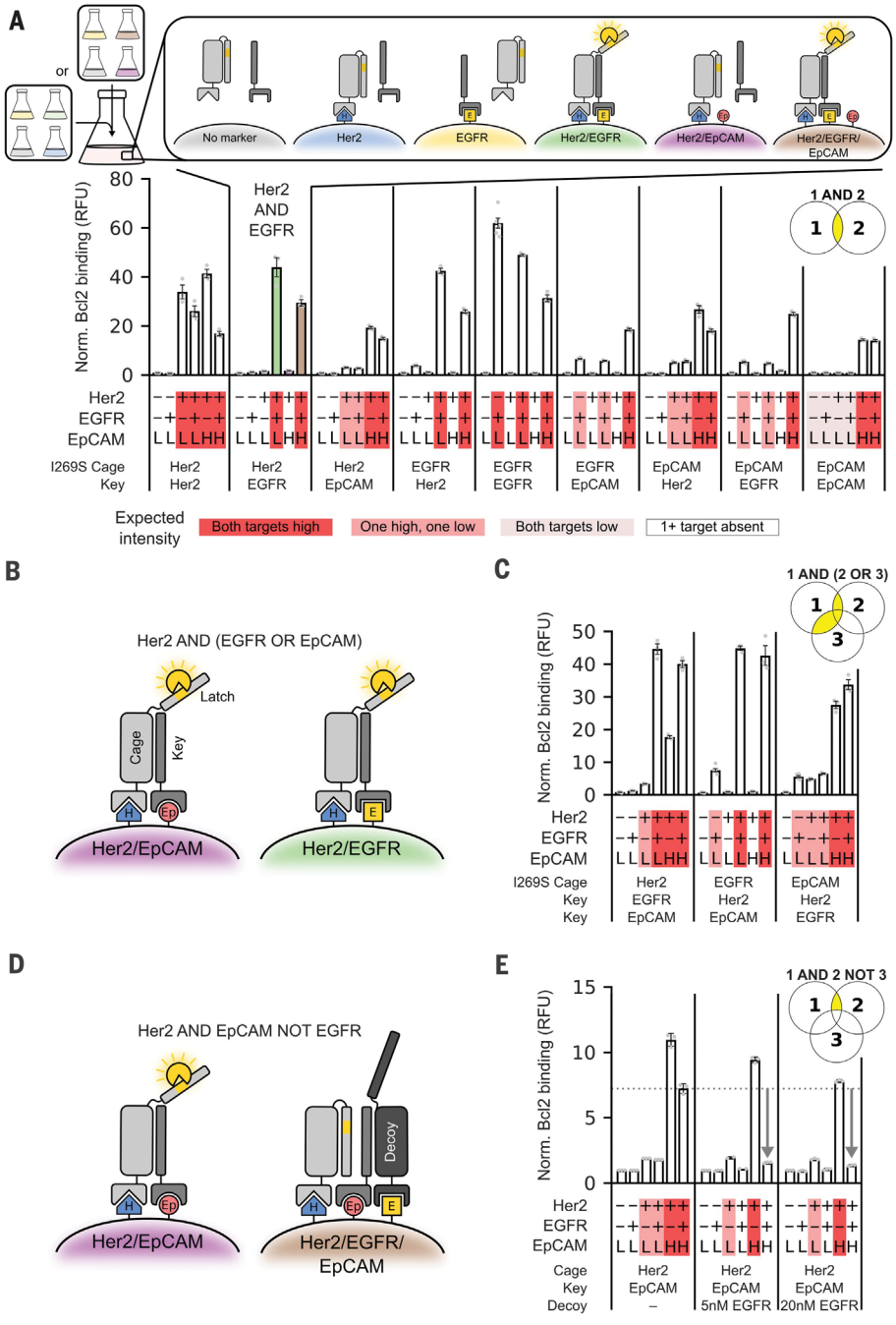

Fig. 3. Co-LOCKR performs two- and three-input logic operations in mixed cell populations. (**A**) Co-LOCKR was used to recruit Bcl2-AF594 in mixed populations of K562 cells expressing different combinations of Her2, EGFR, and EpCAM. Marker expression for each cell line and identity of the cage and key targeting domains are indicated below each bar plot. Red highlighting indicates the expected magnitude of Bcl2-AF594 signal based on relative antigen expression. (**B**) Schematic of [Her2 AND either EGFR OR EpCAM] logic mechanism. (**C**) [Ag_1 AND either Ag_2 OR Ag_3] logic combinations were used to recruit Bcl2-AF594. (**D**) Schematic of [Her2 AND EpCAM NOT EGFR] logic mechanism. The decoy acts as a sponge to sequester the key, thereby preventing cage activation. (**E**) CL_$C_HK_{Ep}D_E$ was used to recruit Bcl2-AF594. Compared with the simple CL_C_HK_{Ep} AND gate (left), recruitment of decoy to EGFR-expressing cells reduced activation to near background levels. For all panels, population 1 was [K562-EpCAM^{lo}, K562-EGFR-EpCAM^{lo}, K562-Her2-EpCAM^{lo}, and K562-Her2-EGFR-EpCAM^{lo}], and population 2 was [K562-EpCAM^{lo}, K562-EGFR-EpCAM^{lo}, K562-Her2-EpCAM^{hi}, and K562-Her2-EGFR-EpCAM^{hi}]. Fluorescence intensities are normalized to the negative control. Error bars represent SEM of six independent replicates for K562 and K562-EGFR and three independent replicates for all others. Statistics are reported in table S4.

chose DARPins as targeting domains to allow facile expression of Co-LOCKR variants, single-chain variable fragments can also be used (fig. S9).

The colocalization-dependent activation mechanism of Co-LOCKR can in principle be extended to include OR logic by adding a second key fused to a targeting domain against an alternative surface marker (Fig. 3B) and NOT logic by adding a decoy protein fused to a targeting domain against a surface marker to be avoided; the decoy acts as a sponge to sequester the key, thereby preventing cage activation (Fig. 3D). Using Her2, EGFR, and EpCAM as model antigens (Ag), we first explored [Ag_1 AND either Ag_2 OR Ag_3] logic on the surface of cells (Fig. 3B). To assess the programmability of Co-LOCKR targeting, we tested all three combinations: [Her2 AND either EGFR OR EpCAM], [EGFR AND either Her2 OR EpCAM], and [EpCAM AND either Her2 OR EGFR]. In all cases, the correct cell subpopulation was targeted at levels consistent with the limiting target antigen (Fig. 3C). For example, CL_$C_EK_HK_{Ep}$ targeted cells expressing EGFR-EpCAM^{lo} 10-fold over background, Her2-EGFR-EpCAM^{lo} 59-fold over background, and Her2-EGFR-EpCAM^{hi} 56-fold above background but did not target cells missing one or more of the antigens (Fig. 3C, middle panel).

We next explored [Ag_1 AND Ag_2 NOT Ag_3] logic using CL_$C_HK_{Ep}D_E$ (D meaning decoy) and the same set of model antigens (Fig. 3D). We tuned the decoy-key affinity with designed point mutations to maximize the abrogation of activation when the decoy is targeted and to minimize the interference of the decoy with activation when it is not targeted (fig. S10). Recruitment of decoy reduced activation to near-background levels on cells with Ag_3 on their surface, while reducing activation on cells lacking Ag_3 by only 15% (Fig. 3E). Consistent with the stoichiometric sequestration mechanism, Ag_3 must be expressed at higher levels than Ag_2 so that the decoy can sequester all molecules of the key (Fig. 3D). While bispecific antibodies can be made to approximate [Ag_1 AND Ag_2] logic by tuning binding affinity, we are not aware of any current approach that can achieve the precise [Ag_1 AND Ag_2 NOT Ag_3] logic of Fig. 3E and fig. S11.

As a first step toward a real-world application, we explored the retargeting of primary human T cell effector function against tumor cells in vitro. We designed a Bcl2 chimeric antigen receptor (CAR) that targets Bim peptides displayed on the surface of a target cell; the CAR contains a stabilized variant of human Bcl2, a flexible extracellular spacer domain (*9*), CD28 and CD3ζ signaling domains, and a truncated EGFR (EGFRt) selection marker (*10*) linked by a T2A ribosomal skipping sequence (fig. S12A). The Bcl2 CAR functions as designed:

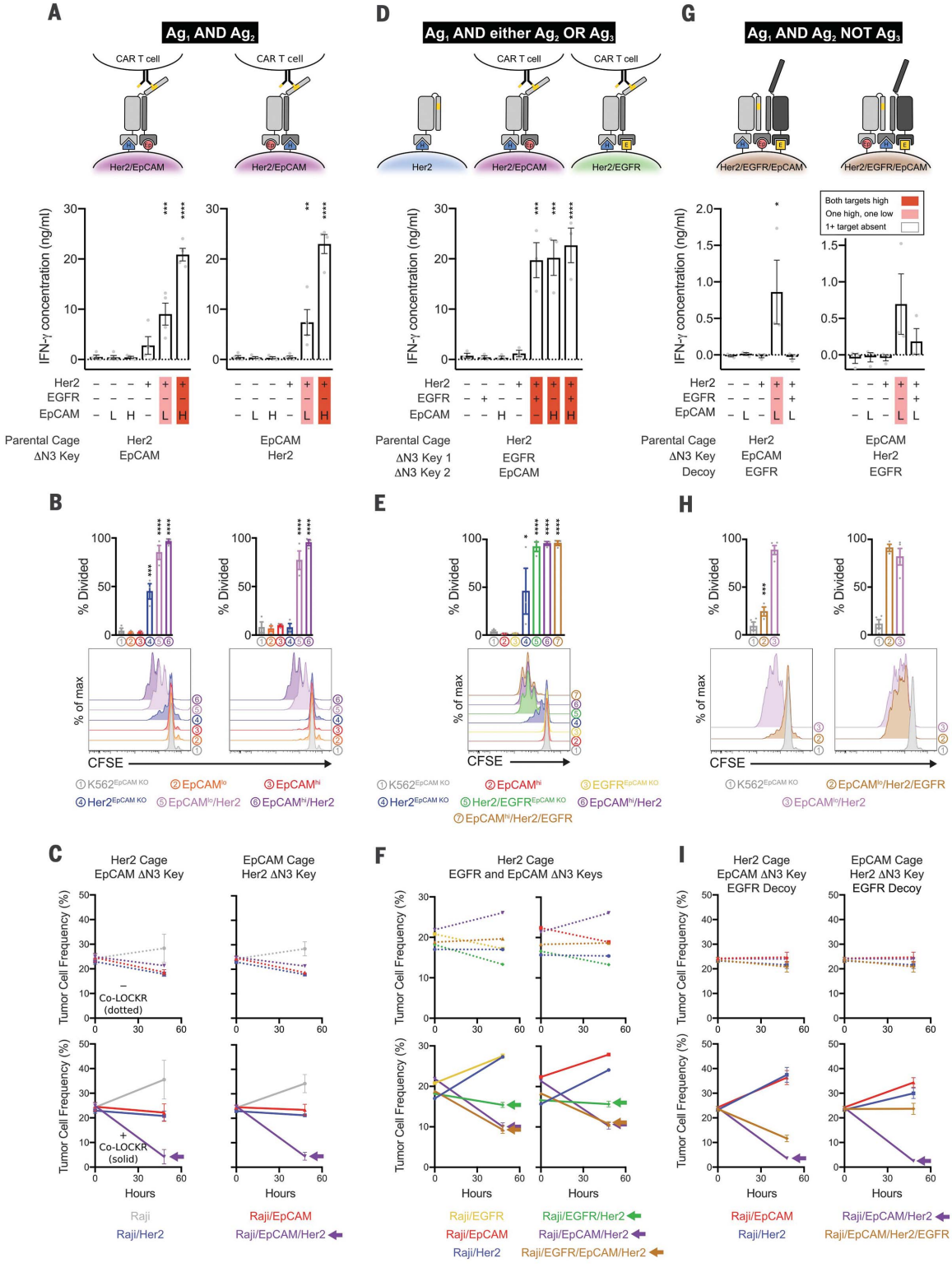

Fig. 4. Co-LOCKR directs CAR T cell specificity using two- and three-input logic operations. (**A**, **D**, and **G**) Mean IFN-γ concentration in cell supernatants 24 hours after coculture of cage, key, and K562 cells with CAR T cells. Marker expression for each cell line and identity of the cage and key targeting domains are indicated below each bar plot. Red highlighting indicates the expected magnitude of signal based on the target cell's relative antigen expression. Error bars represent SEM of $n = 4$ (A) or 3 [(D) and (G)] healthy T cell donors. AND/NOT logic is demonstrated with EpCAM^{lo} target K562 cells because T cell effector function was leaky for EpCAM^{hi} target cells (see fig. S15A). (**B**, **E**, and **H**) CAR T cell proliferation in response to [Her2 AND EpCAM] (B), [Her2 AND EGFR OR EpCAM] (E), or [Her2 AND EpCAM NOT EGFR] (H) logic. Bar plots are the percent of T cells that have undergone at least one cell division by 72 hours after coculture of CAR T cells, cage, key, and target K562 cells. Histograms show flow cytometric analysis of CFSE (carboxyfluorescein succinimidyl ester) dye dilution gated on CD8$^+$ lymphocytes. The data are representative of $n = 3$ biological replicates with healthy T cell donors. (**C**, **F**, and **I**) CAR T cell cytotoxicity against mixed populations of target Raji cells expressing combinations of Her2, EGFR, and EpCAM. Line graphs show mean frequency of Raji target cells after 0 or 48 hours of coculture with CAR T cells. $n = 4$ [(C) and (F)] or 3 (I) healthy donors. Arrows indicate cell lines targeted by Co-LOCKR.

Purified CD8$^+$EGFRt$^+$ Bcl2 CAR T cells efficiently recognized K562 cells stably expressing a surface-exposed Bim-GFP fusion protein (fig. S12, B and C).

With Bcl2 CAR T cells in hand, we investigated whether the Co-LOCKR proteins could mediate T cell activation by Raji and K562 cells expressing combinations of Her2, EGFR, and EpCAM. The Raji cells expressed lower levels of transduced antigens than did the K562 cell lines (fig. S7 and table S3) and hence more stringently test Co-LOCKR sensitivity, whereas the K562

cells better assess specificity. CL_C_HK_{Ep} and CL_$C_{Ep}K_H$ (using the parental unmutated cage) promoted interferon-γ (IFN-γ) release only when cocultured with Raji-Her2-EpCAM cells and not Raji-EpCAM or Raji-Her2 cells (fig. S12D). Titration experiments showed that CAR T effector function could be specifically targeted using between 2.5 nM and 20 nM of Co-LOCKR without causing unintended activation by off-target cells (fig. S13); even lower concentrations would likely be effective using higher-affinity binding domains.

Next, we assessed the ability of Co-LOCKR to direct CAR T cell cytotoxicity against specific subsets of cells within a mixed population. Raji, Raji-EpCAM, Raji-Her2, and Raji-Her2-EpCAM were differentially labeled with fluorescent CellTrace dyes and mixed together with CAR T cells and CL_C_HK_{Ep} (fig. S12F), and killing of each of the cell lines was assessed using flow cytometry. After 48 hours, Raji-Her2-EpCAM cells were preferentially killed, but a fraction of Raji-EpCAM cells were also targeted (fig. S12G), suggesting that even the parental cage and key were too leaky for CAR T cell recruitment. We overcame this basal activation by modifying the length of the key (fig. S12E): The combination of parental cage and ΔN3 key (three N-terminal amino acids deleted) selectively targeted Raji-Her2-EpCAM cells and mitigated unintended killing of Raji-EpCAM and Raji-Her2 cells (fig. S12, F and G). A chromium release assay showed that CL_C_HK_{Ep} targeted only Raji-Her2-EpCAM cells and initiated rapid cell killing within 4 hours (fig. S12H). Thus, Co-LOCKR can be used to restrict IFN-γ release and cell killing to only those tumor cells that express a specific pair of antigens.

We next evaluated Co-LOCKR AND logic for additional tumor antigen pairs ([Her2 AND EpCAM] and [Her2 AND EGFR]) and varying antigen density profiles using K562 cell lines (fig. S7A and table S3) and solid tumor lines (fig. S8A). Raji cells with low antigen density yielded modest IFN-γ (fig. S14A), K562-Her2-EpCAM^{lo} and SKBR3 breast cancer cells yielded intermediate IFN-γ (Fig. 4A and fig. S14B), and both K562-Her2-EpCAM^{hi} and K562-Her2-EGFR cells yielded high IFN-γ release for their respective Co-LOCKRs (Fig. 4A and fig. S14C). CL_$C_{Ep}K_H$ induced IFN-γ release in response to Raji-Her2-EpCAM 3.9-fold above background; SKBR3, 4.8-fold above background; K562-Her2-EpCAM^{lo}, 16-fold above background; and K562-Her2-EpCAM^{hi}, 51-fold above background, with minimal off-target cytokine release. IFN-γ production did not increase appreciably when the target cells expressed high levels of a single antigen. CAR T cells proliferated only upon coculture with target cells coexpressing the correct pair of antigens, and the degree of proliferation positively correlated with antigen density (Fig. 4B and fig. S14D). The flow cytometry–based killing assay demonstrated AND gate selective cytotoxicity with both CL_C_HK_{Ep} and CL_$C_{Ep}K_H$ against Raji-Her2-EpCAM without depleting single antigen–positive cells (Fig. 4C). A similar result was observed for both CL_C_HK_E and CL_C_EK_H against Raji-Her2-EGFR (fig. S14E), although killing was less effective, likely because of the lower expression levels of EGFR compared with EpCAM in Raji-Her2-EGFR and Raji-Her2-EpCAM, respectively. Additionally, we did not observe fratricide of the EGFRt$^+$ CAR T cells used in the experiment, which could have been targeted by the anti-EGFR DARPin (fig. S14F).

Encouraged by robust AND logic, we evaluated more complex operations involving combinations of AND and either OR or NOT logic. CAR T cells cocultured with AND/OR Co-LOCKRs (CL_$C_HK_EK_{Ep}$, CL_$C_EK_HK_{Ep}$, and CL_$C_{Ep}K_HK_E$) each carried out [Ag_1 AND either Ag_2 OR Ag_3] logic with respect to IFN-γ production (Fig. 4D and fig. S14G) and proliferation (Fig. 4E) against K562 cell lines, as well as selective killing in a mixed population of Raji cell lines (Fig. 4F and fig. S14H). CAR T cells cocultured with an AND/NOT Co-LOCKR (CL_$C_HK_{Ep}D_E$) carried out [Her2 AND EpCAM NOT EGFR] logic: IFN-γ production and proliferation were induced in the presence of K562-Her2-EpCAM^{lo} but not K562-Her2-EGFR-EpCAM^{lo} cells (Fig. 4, G and H). Consistent with the observations above, Ag_3 in the NOT operation had to be expressed at higher levels than Ag_2 (Fig. 4, G to I, and fig. S15). While these data indicate that careful antigen selection and some tuning are necessary for robust control of logical operations, the ability of CL_$C_{Ep}K_HD_E$ to direct CAR T cell mediated killing of Her2$^+$EpCAM$^+$ cells but not Her2$^+$EGFR$^+$EpCAM$^+$ cells (Fig. 4I, right-hand panel) further highlights the power of Co-LOCKR to perform [Ag_1 AND Ag_2 NOT Ag_3] logic for specific cell targeting.

Two previous strategies improved the specificity of CAR T cells by approximating AND logic. First, Kloss *et al.* (*11*) directly modulated signaling from a suboptimally activating first generation CAR (CD3ζ only) using a chimeric costimulatory receptor (CCR; costimulatory domain only) that recognizes a distinct second antigen. Although T cell activation is reduced in the absence of the second antigen, targeting remains leaky because the CAR T cells can lyse both tumor and normal cells expressing the antigen targeted by the CD3ζ CAR, even when the CCR is not engaged. Second, Morsut *et al.* (*12*) developed synthetic Notch receptors that modularly induce expression of effector proteins in engineered cells. Roybal *et al.* (*13*) applied this technology to enhance CAR T cell specificity using a synthetic Notch receptor that upon engaging one antigen induces expression of a CAR recognizing a second antigen. Although this if-then logic strategy has shown promise in preclinical models in which the target antigens exist distally, the CAR will kill any nearby cell expressing the target antigen, so off-tumor toxicity can occur when the Notch receptor and CAR targets are expressed in neighboring healthy tissues (*14*). Co-LOCKR has potential advantages over these approaches, as activation requires binding in cis to a precise combination of target antigens before recruiting the cognate CAR T cells, and thus it can direct killing without harming neighboring off-target cells displaying single antigens (Fig. 4, C, F, and I). OR (*15*, *16*) and NOT (*15*, *17*) logic has also been described for CAR T cells, but not in combination with AND logic as described here.

Our CAR T cell experiments demonstrate the potential for Co-LOCKR to mediate targeting specificity in vitro; however, several additional challenges will have to be met for Co-LOCKR to be a clinically translatable therapeutic. In vivo studies will be needed to assess and improve the pharmacokinetics of the Co-LOCKR components. Immunogenicity of the designed proteins is also a potential concern, as with any other system comprising nonhuman proteins. As Co-LOCKR actuation is thermodynamically controlled, the therapeutic index will depend on the affinity of the targeting domains used to direct the Co-LOCKR proteins to antigens on the target cells: If the affinities are subnanomolar, dosing can be far below the 40-nM level where activation starts to occur in solution (fig. S13). CAR T efficacy could also be improved by optimizing the CAR, for example, by using alternative signaling molecules (*18*–*20*).

The power of Co-LOCKR results from the integration of multiple coherent or competing inputs that determine the magnitude of a single response. The output signal—exposure of the functional peptide on the latch—is increased by key binding and countered by decoy competition. Thus, the proteins can intrinsically perform logic rather than relying on cellular machinery for signal integration. Although our present work has focused on development of the Co-LOCKR system and CAR T cell applications, the Co-LOCKR system should be powerful for engineering biology in any setting that requires proximity-based activation or targeting of specific subpopulations of cells.

REFERENCES AND NOTES

1. C. Sellmann *et al.*, *J. Biol. Chem.* **291**, 25106–25119 (2016).
2. Y. Mazor *et al.*, *Sci. Rep.* **7**, 40098 (2017).
3. R. A. Langan *et al.*, *Nature* **572**, 205–210 (2019).
4. S. E. Boyken *et al.*, *Science* **352**, 680–687 (2016).
5. A. Leaver-Fay *et al.*, *Methods Enzymol.* **487**, 545–574 (2011).

6. L. Delgado-Soler, M. Pinto, K. Tanaka-Gil, J. Rubio-Martinez, *J. Chem. Inf. Model.* **52**, 2107–2118 (2012).
7. C. Zahnd *et al*., *J. Mol. Biol.* **369**, 1015–1028 (2007).
8. D. Steiner, P. Forrer, A. Plückthun, *J. Mol. Biol.* **382**, 1211–1227 (2008).
9. M. Hudecek *et al*., *Cancer Immunol. Res.* **3**, 125–135 (2015).
10. X. Wang *et al*., *Blood* **118**, 1255–1263 (2011).
11. C. C. Kloss, M. Condomines, M. Cartellieri, M. Bachmann, M. Sadelain, *Nat. Biotechnol.* **31**, 71–75 (2013).
12. L. Morsut *et al*., *Cell* **164**, 780–791 (2016).
13. K. T. Roybal *et al*., *Cell* **164**, 770–779 (2016).
14. S. Srivastava *et al*., *Cancer Cell* **35**, 489–503.e8 (2019).
15. J. H. Cho, J. J. Collins, W. W. Wong, *Cell* **173**, 1426–1438.e11 (2018).
16. E. Zah, M.-Y. Lin, A. Silva-Benedict, M. C. Jensen, Y. Y. Chen, *Cancer Immunol. Res.* **4**, 498–508 (2016).
17. V. D. Fedorov, M. Themeli, M. Sadelain, *Sci. Transl. Med.* **5**, 215ra172 (2013).
18. S. Tammana *et al*., *Hum. Gene Ther.* **21**, 75–86 (2010).
19. Y. Kagoya *et al*., *Nat. Med.* **24**, 352–359 (2018).
20. C. Sun *et al*., *Cancer Cell* **37**, 216–225.e6 (2020).

ACKNOWLEDGMENTS

We thank A. Scharenberg, W. Lim, R. Klausner, L. Stewart, A. Roy, Z. Chen, A. Briggs, E. Gray, D. Stetson, M. Pepper, L. Carter, B. Weitzner, J. Pearl, H. Moffett, I. Haydon, D. Campbell, S. Hauschka, N. King, and J. Zalatan for helpful advice; D. Prunkard and H. Nguyen for technical assistance with flow cytometry and cell sorting; A. Kang for setting up crystal trays and looping crystals; R. Ravichandran for protein purification; and S. Berger for sharing biotinylated Bcl2, D. Hockenbery for sharing SKBR3 cells, and D. Trono for sharing lentiviral packaging plasmids. We also thank the W. M. Keck Center for Advanced Studies in Neural Signaling (NIH grant S10 OD016240) and the helpful input of N. Peters and G. Liu for confocal microscopy experiments. **Funding:** This work was supported by the HHMI (D.B.), the Open Philanthropy Project (D.B.), the NSF (D.B., CHE-1629214), the DTRA (D.B., HDTRA1-18-1-0001), the Nordstrom Barrier IPD Directors Fund (D.B.), the Washington Research Foundation and Translational Research Fund (D.B.), the Audacious Project organized by TED (D.B.), and the NIH (S.R.R., R01 CA114536; J.B., NIGMS T32GM008268). M.J.L. was supported by a Washington Research Foundation Innovation Postdoctoral Fellowship and a Cancer Research Institute Irvington Fellowship from the Cancer Research Institute. S.E.B. was supported by the Burroughs Wellcome Fund Career Award at the Scientific Interface. A.I.S. was supported by the FHCRC interdisciplinary training grant in cancer research and Hearst Foundation. A.O. was supported by NIH NCI grants 1R21CA232430-01 and T32CA080416. **Author contributions:** M.J.L., S.E.B., A.I.S.: Conceptualization, Methodology, Investigation, Software, Data analysis, Writing – original draft, Writing – review and editing, Visualization, and Supervision. J.B.: Investigation, Data analysis, Writing – original draft, Writing – review and editing, and Visualization. A.R.: Investigation. R.A.L.: Investigation and Software. A.O.: Methodology, Investigation, Software, Data analysis, and Visualization. V.M.: Investigation. M.J.B.: Investigation, Software, and Data analysis. M.G., A.Q.-R., J.J., G.L., A.N.: Investigation. S.P., C.E.C., S.R.R.: Supervision. D.B.: Conceptualization, Writing – original draft, Writing – review and editing, Visualization, and Supervision. M.J.L., S.E.B., and D.B. conceived of the study. M.J.L., S.E.B., A.I.S., J.B., and A.O. designed the experiments. M.J.L., S.E.B., and R.A.L. designed the LOCKR proteins. M.J.L., A.I.S., A.R., and M.G. made the target cell lines. M.J.L., S.E.B., J.B., R.A.L., A.Q.-R., J.J., G.L., and A.N. performed cloning, protein expression, and biochemical characterization experiments. S.E.B. and M.J.B. solved the crystal structure. M.J.L., J.B., and A.O. quantified Co-LOCKR activation using flow cytometry. A.O. performed the microscopy experiment and data analysis. A.I.S., A.R., and V.M. performed the T cell experiments. M.J.L., S.E.B., A.I.S., J.B., R.A.L., A.O., and M.J.B. analyzed the data. M.J.L., S.E.B., A.I.S., S.P., C.E.C., S.R.R., and D.B. supervised the study. M.J.L., S.E.B., A.I.S., and D.B. wrote the manuscript. All authors reviewed the manuscript and provided feedback. **Competing interests:** M.J.L., S.E.B., A.I.S., J.B., R.A.L., M.G., C.E.C., S.R.R., and D.B. are inventors on patents related to this work. M.J.L., S.E.B., A.I.S., R.A.L., M.J.B., S.R.R., and D.B. hold equity in Lyell Immunopharma. D.B. holds equity in Sana Biotechnology. M.J.L., S.E.B., R.A.L., M.J.B., and S.R.R. are employees of Lyell Immunopharma. A.I.S. is a consultant of Lyell Immunopharma. **Data and materials availability:** Coordinates and structure files have been deposited to the Protein Data Bank (PDB) under ID 7JH5. The python script used to analyze confocal microscopy images is included in the supplemental material. Expression plasmids and cell lines are available upon request. Primary T cells are not available.

SUPPLEMENTARY MATERIALS

science.sciencemag.org/content/369/6511/1637/suppl/DC1
Materials and Methods
Figs. S1 to S21
Tables S1 to S5
Supplementary Scripts
References (*21*–*33*)
MDAR Reproducibility Checklist

View/request a protocol for this paper from *Bio-protocol*.

20 December 2019; accepted 28 July 2020
Published online 20 August 2020
10.1126/science.aba6527